LIBERTAS MATHEMATICA, vol XXXI (2011)

An Innovative Method for Non-linear Image Registration

M. AKINLAR, M. CHU, Y. GONG, S. HSIAO, C. HSIEH, G. LIAO and S. SALAKO

Abstract. In this paper we present numerical implementation of a new variational approach to non-rigid registration of images. Our method is based on adjusting divergence and curl of image displacement field, which determines pixel correspondences. An image registration procedure might be decomposed into three major components: the problem statement, the registration paradigm and the optimization procedure. Our method minimizes a similarity metric such as the sum of squared differences and uses Lagrange multipliers method to solve the optimization problem governed by the divergence and curl equations. In our implementation, the minimization problem is reduced to solving Poisson equations. A finite-difference multigrid strategy is used to solve these Poisson equations. Computational experiments demonstrate the promising potential of our registration method.

Keywords: image registration, Lagrange multipliers, multigrid Poisson solver.

1 Introduction

Non-linear image registration is a highly nonlinear process of establishing pixel-by-pixel correspondences between two (or more) "similar" images. The images could be of the same or different objects and imaging modalities. They can possibly be taken at different distances, angles and times. In fact, image registration can be described as finding a spatial transformation between pixels (or voxels) of two images that maximizes a similarity measure called the data term between the two images.

In general the image registration problem is an ill-posed optimization problem. A large class of current variational techniques can be formulated as an regularized optimization problem:

$$\mathcal{J}[\mathbf{R}, \mathbf{T}; u] := \min \{C_{sim} + \beta C_{reg}\}, \tag{1.1}$$

where C_{sim} is the similarity metric between template and reference images, $\mathbf{T}$ and $\mathbf{R}$, respectively; and C_{reg} is a regularizing term; β is a weighting parameter. Typical regularization terms are fluid-like, elastic, diffusive, or curvature-based smoothers. Let us note that adding a regularization term may affect the quality of the registration in a negative manner. Some drawbacks by adding a regularization term to the cost functional are: (i) The resulting

transformations depend on the nature of the regularizing term, which may impose unrealistic physical properties. (ii) If the regularity constant β is too small, the regularity will not be strong enough and the algorithm will be unstable. (iii) If β is too large, the regularity will be too strong and the resulting transformations will not optimize the similarity measure accurately.

We can desribe the image registration problem as an algorithm that consists of three components:

- **Transformation models:** Rigid (affine, global), non-rigid (non-linear and local), hybrid.
- **Similarity measures:** Intensity-based, features-based.
- **Optimization methods:** Lagrange multipliers method.

An image registration is called **rigid**, if only rotations, translations, projections, scaling are envolved. In the literature rigid transformations have found application areas in orthopedic imaging because of the rigid-transformations do not consider soft tissue deformations. Bone growth can be given as a specific example for rigid image registration. If the image transformation maps lines onto curves, it is called **non-rigid**. Non-rigid image registration is an essential tool required for overcoming, for example, soft tissue deformations in medical images. Non-rigid registrations are mostly local and are not linear, so they can not be represented by means of matrices. The most well-known non-rigid image registrations types are the elastic model proposed by [2], diffusion image registration [15], viscous fluid model proposed by Christensen [3], and curverture based image registration [4]. Let us note that our method can handle certain amount of deformation in 2D images by divergence and curl which makes our method non-rigid.

Detecting tumors, locating diseased areas, image fusion, feature matching and motion tracking are some of the important applications of the image registration problem. Image registration is an important and challenging subject which usually involves high storage requirements, high CPU costs, finding reliable similarity measures, noisy and distorted data in medical images, occlusion and "ill-posed" optimization problems. Therefore finding reliable image registration techniques are significant subject of image processing. Unfortunately, no general theory for image registration has been yet established.

Landmark-based registration, Cross-correlation, thin plate spline interpolation, sum of squared differences, mutual information, segmentation-based registration [6] are some of the popular image registration techniques. It appears that each application has developed its own approaches and implementation depending on the particular application.

[9] presented a method of diffeomorphic image registration using the method of discrete mechamics and optimal control.

[14] presented a multi-start multi-resolution parallel registration algorithm for accurate alignment of BSEM (Back-Scattered Scanning Electron Microscopy) and micro-CT image pairs.

In this paper we continue investigation of a new image registration method proposed in [11]. The sum of squared differences (SSD) is employed as the similarity measure in the cost minimization of the existing registration framework.

We use Lagrange multipliers method to derive an optimality system which consists of state equations, costate equations, and optimality conditions.

We apply these techniques to several computational examples. Our results show that the method is very promising.

In [11], a least square finite element method is used to solve the optimality system, but no medical image examples are demonstrated. In this paper, a simpler finite difference method with multigrid Poisson solver is used, and real medical images from the Visible Human Project [1] are registered.

Some merits of our method are listed as follows:

- It is based on a solid mathematical foundation [11, 12]. In particular, it accounts for local volume changes through the divergence of the transformation; and it accounts for local rotation through the curl vector of the transformation.
- The method is based on a linear differential system; its numerical implementation is fast, stable and simple.
- The method is general in the sense that it may be used in any optimization problem that involves motion estimation. Thus, it has the potential to be the numerical kernel for a wide range of applications.

This paper is organized as follows. In the first section we overview the ideas and methodology behind the image registration. In Section 2 we present our method to non-rigid registration of 2D images. We express the image registration problem as an optimization problem and use the sum of squared difference as the similarity metric. Using Lagrange multipliers method we obtain the optimality system which consists of state, co-state equations and optimality conditions. From the optimality system we get four Poisson equations in the same section. In Section 3 we describe an iterative numerical scheme for the solution of these Poisson equations. Computational examples are reported in Section 4. Summary and conclusion are presented in the last section.

2 Our Method for 2D Image Registration

Given a *reference image* $\mathbf{R}(\mathbf{x})$ and a *template image* $\mathbf{T}(\mathbf{x})$, we define the image registration problem as an optimization problem: find a mapping $\boldsymbol{\phi}(\mathbf{x})$ that minimizes the L^2-norm of the difference between $\mathbf{T}\big(\boldsymbol{\phi}(\mathbf{x})\big)$ and $\mathbf{R}(\mathbf{x})$ over Ω. Figure 1 contains an example for a reference and template image. It is seen in Figure 1 that the image on the right hand side is bigger than the one on the left hand side and the one on the right hand side is rotated clockwise with a certain angle. In our image registration method we use divergence and curl to model the free-form deformation between the images. We define the image registration deformation by

$$\phi(\mathbf{x}) \;=\; \mathbf{x} + u(\mathbf{x}) \;=\; (\phi_1(\mathbf{x}), \phi_2(\mathbf{x})) \;=\; (x_1 + u_1(\mathbf{x}), x_2 + u_2(\mathbf{x}))$$

where $u(\mathbf{x}) = (u_1(\mathbf{x}), u_2(\mathbf{x}))$ is the displacement field and $\mathbf{x} = (x_1, x_2) \in \mathbf{R}^2$. Let us define Jacobian determinant of the image registration mapping $\boldsymbol{\phi}(\mathbf{x})$ as $f(\mathbf{x})$. Following theorem establishes a relationship between the image registration map $\boldsymbol{\phi}(\mathbf{x}) = \mathbf{x} + u(\mathbf{x})$ and $f(\mathbf{x})$.

Theorem 1 *Let $\Omega \subset \mathbf{R}^2$ be a domain. For $\boldsymbol{\phi}(\mathbf{x}) = \mathbf{x} + \varepsilon u(\mathbf{x})$, the equality $J(\boldsymbol{\phi})(\mathbf{x}) \cong 1 + div\,(\varepsilon u(\mathbf{x})) + O(\varepsilon^2)$ holds for every $\varepsilon > 0$ in Ω where $J(\boldsymbol{\phi})(\mathbf{x})$ is the Jacobian determinant of $\boldsymbol{\phi}(\mathbf{x})$.*

Proof.

$$J(\phi)(\mathbf{x}) = \begin{vmatrix} 1+\varepsilon u_{1_{x_1}}(\mathbf{x}) & \varepsilon u_{1_{x_2}}(\mathbf{x}) \\ \varepsilon u_{2_{x_1}}(\mathbf{x}) & 1+\varepsilon u_{2_{x_2}}(\mathbf{x}) \end{vmatrix} = 1 + div\,(\varepsilon u(\mathbf{x})) + O(\varepsilon^2)$$

from which we obtain

$$div\, u(\mathbf{x}) \;=\; f(\mathbf{x}) - 1$$

by ignoring the ε^2 terms and denoting εu by u.

Next we present our optimal control approach to the non-rigid registration of 2D images. We want to minimize the cost functional

$$\mathcal{J}(\boldsymbol{\phi}, f, \mathbf{g}) = \frac{1}{2}\int_\Omega \left|\mathbf{T}\big(\boldsymbol{\phi}(\mathbf{x})\big) - \mathbf{R}(\mathbf{x})\right|^2 d\mathbf{x} \tag{2.2}$$

subject to

$$\begin{aligned} div\, u(\mathbf{x}) &= f(\mathbf{x}) - 1 \quad \text{on} \quad \Omega \\ curl\, u(\mathbf{x}) &= g(\mathbf{x}) \quad \text{on} \quad \Omega \\ u(\mathbf{x}) &= 0 \quad \text{on} \quad \partial\Omega, \end{aligned} \tag{2.3}$$

where $u(\mathbf{x})$ is the displacement between pixels in template and reference images and $\partial\Omega$ is the boundary of Ω, and $f(\mathbf{x})$ and $g(\mathbf{x})$ are control functions to be determined by the optimization procedure. $f(\mathbf{x})$ is related to the Jacobian determinant and is chosen as 1 initially. $g(\mathbf{x})$ is related to the curl of the displacement field and is chosen as 0 initially.

Though in (2.2), w_i, $i = 1, 2$, are penalty weights, this does not mean that we are using a regularization term. These penalty weights are used only to control the image nodes in the domain of interest during the movement of pixels.

Note:

1. The constraint (2.3) is a linearized version of the moving grid deformation method [13].
2. In [10], another simplified version of the deformation method is used as constraint.

Implementation 1 We use the Lagrange multiplier method to transform the constrained minimization problem into an unconstrained saddle point problem. To this end, we introduce the Lagrange multipliers $v_1(\mathbf{x})$ and $v_2(\mathbf{x})$ and define the Lagrangian functional

$$\begin{aligned} \mathcal{L}(\boldsymbol{\phi}, f, \mathbf{g}) &= \frac{1}{2}\int_\Omega \left|\mathbf{T}\big(\boldsymbol{\phi}(\mathbf{x})\big) - \mathbf{R}(\mathbf{x})\right|^2 d\mathbf{x} + \frac{w_1}{2}\int_\Omega |f(\mathbf{x})|^2\, d\mathbf{x} \\ &+ \frac{w_2}{2}\int_\Omega |g(\mathbf{x})|^2\, d\mathbf{x} + \int_\Omega v_1(\mathbf{x})(div\, u(\mathbf{x}) - f(\mathbf{x}) + 1)d\mathbf{x} \\ &+ \int_\Omega v_2(\mathbf{x})(curl\, u(\mathbf{x}) - g(\mathbf{x}))d\mathbf{x} \end{aligned}$$

Solution of the Lagrange functional satisfies the optimality system which consists of state equations, costate equations, and the optimality conditions. The constraint (2.3) is explicitly substituted into (2.2) and the state and co-state functions are required to satisfy

$\mathbf{u} = \mathbf{0}$ and $\mathbf{v} = \mathbf{0}$, respectively. Saddle points of Lagrangian functional satisfy an optimality system that consists of state equations, co-state equations, and optimality conditions; the optimality system is obtained from the first-order necessary conditions for the stationarity of $\mathcal{L}$.

Specializing an abstract theorem concerning the existence of Lagrange multipliers for minimizations on Banach space [16], we obtain the following theorem:

Theorem 2 *Let V_1 and V_2 be two Hilbert spaces, $\mathcal{F}$ a functional on V_1, and $\mathcal{G}$ a mapping from V_1 to V_2. Assume $\hat{u}$ is a solution of the following constrained minimization problem:*

Find $u \in V_1$ that minimizes $\mathcal{F}(u)$ subject to $\mathcal{G}(u) = 0$. Assume further that the following conditions are satisfied:

(i) $\mathcal{F} : Nbhd(\widehat{u}) \subset V_1 \to \mathbf{R}$ is Frechet-differentiable at $\widehat{u}$;

(ii) $\mathcal{G}$ is continuously Frechet-differentiable at $\widehat{u}$;

(iii) $\mathcal{G}'(\widehat{u}) : V_1 \to V_2$ is onto.

Then, there exists a $\mu \in (V_2)^*$ such that

$$\mathcal{F}'(\widehat{u})v - \langle \mu, \mathcal{G}'(\widehat{u})v \rangle = 0, \qquad \forall v \in V_1.$$

Proof. See [16], Theorem 43.19. Here, $\langle \cdot, \cdot \rangle$ denotes the duality pairing between V_2 and $(V_2)^*$ and $\mathcal{F}'(\widehat{u})v$ and $\mathcal{G}'(\widehat{u})v$ denote the actions of $\mathcal{F}'(\widehat{u})$ as an operator mapping $v \in V_1$ into $\mathbf{R}$ and $\mathcal{G}'(\widehat{u})$ as an operator mapping $v \in V_1$ into V_2, respectively.

We will fit our optimization problem into the above abstract framework. A related work for the use of Lagrange multiplier method and the existence of solutions of the optimality system can be seen at [5] for a similar optimal control problem. Next we obtain optimality system which consists of state, co-state equations and optimality conditions.

State Equations: The state equations are obtained from $\mathcal{L}_{v_1} = 0, \quad \mathcal{L}_{v_2} = 0$, where $\mathcal{L}_{v_i}$ represent the Fréchet derivative of $\mathcal{L}$ with respect to v_i for $i = 1, 2$.

$$\begin{aligned} \mathcal{L}_{v_1} &= \frac{d}{d\varepsilon}\Big|_{\varepsilon=0} \mathcal{L}[v_1 + \varepsilon\delta v_1] = \frac{d}{d\varepsilon}\Big|_{\varepsilon=0} \int_\Omega (v_1 + \varepsilon\delta v_1)(div\, u - f + 1) \\ &= \int_\Omega \delta v_1 (div\, u - f + 1) = 0 \quad \text{for every} \quad \delta v_1. \end{aligned}$$

Then, the first state equation is

$$div\, u(\mathbf{x}) = f(\mathbf{x}) - 1. \tag{2.4}$$

In the similar way, by solving the equation $\mathcal{L}_{v_2} = 0$ we obtain the second state equation as

$$curl\, u(\mathbf{x}) = g(\mathbf{x}). \tag{2.5}$$

Costate Equations: The costate equations are obtained by solving the equations $\mathcal{L}_{u_1} = 0, \;\; L_{u_2} = 0$.

$$\begin{aligned}
\mathcal{L}_{u_1} &= \frac{d}{d\varepsilon}\Big|_{\varepsilon=0}\Big[\frac{1}{2}\int_\Omega [\mathbf{T}(\mathbf{x}+(u_1(\mathbf{x})+\varepsilon\delta u_1(\mathbf{x}),u_2(\mathbf{x})))-\mathbf{R}(\mathbf{x})]^2 \\
&+ \int_\Omega v_1(div\,(u_1+\varepsilon\delta u_1,u_2)-f+1)+\int_\Omega v_2(curl\,(u_1+\varepsilon\delta u_1,u_2)-g)\Big] \\
&= \int_\Omega (\mathbf{T}(\mathbf{x}+u(\mathbf{x}))-\mathbf{R}(\mathbf{x}))\,\mathbf{T}_{\phi_1}\,\delta u_1+\int_\Omega v_1(\delta u_1)_{x_1}+\int_\Omega v_2(-\delta u_1)_{x_2} \\
&= \int_\Omega (\mathbf{T}(\mathbf{x}+u(\mathbf{x}))-\mathbf{R}(\mathbf{x}))\,\mathbf{T}_{\phi_1}\,\delta u_1+\int_\Omega (v_1,-v_2)\cdot\nabla\delta u_1 \\
&= \int_\Omega [(\mathbf{T}-\mathbf{R})\,\mathbf{T}_{\phi_1}\,\delta u_1-\nabla\cdot(v_1,-v_2)\delta u_1]\ \text{(by Gauss theorem)} \\
&= \int_\Omega [(\mathbf{T}-\mathbf{R})\,\mathbf{T}_{\phi_1}-\nabla\cdot(v_1,-v_2)]\,\delta u_1=0 \text{ for every } \delta u_1,
\end{aligned}$$

which gives us the first costate equation

$$\nabla\cdot(v_1,-v_2)=(\mathbf{T}-\mathbf{R})\mathbf{T}_{\phi_1}. \tag{2.6}$$

In the similar manner, from the equation $\mathcal{L}_{u_2}=0$ we obtain the second costate equation as

$$\nabla\cdot(v_2,v_1)=(\mathbf{T}-\mathbf{R})\mathbf{T}_{\phi_2}. \tag{2.7}$$

Optimality conditions: The optimality conditions are obtained by solving the equations $\mathcal{L}_f=0,\ \mathcal{L}_g=0$.

$$\begin{aligned}
\mathcal{L}_f &= \frac{d}{d\varepsilon}\Big|_{\varepsilon=0}\left[\frac{w_1}{2}\int_\Omega (f+\varepsilon\delta f)^2+\int_\Omega v_1(div\,u-(f+\varepsilon\delta f)+1)\right] \\
&= \int_\Omega w_1\,f\delta f-v_1\delta f \\
&= \int_\Omega (w_1\,f-v_1)\delta f=0 \text{ for every } \delta f,
\end{aligned}$$

which gives us the first optimality condition

$$w_1\,f=v_1. \tag{2.8}$$

By solving $\mathcal{L}_g=0$ we get the second optimality condition as

$$w_2\,g=v_2. \tag{2.9}$$

In order to solve these system of equations we write a coupling system and then solve the resulting Poisson equations by an iterative way in a decoupled manner. Define $G:=(G_1,G_2)$ as

$$\begin{aligned}
G_1 &:= (\mathbf{T}-\mathbf{R})\mathbf{T}_{\phi_1}, \\
G_2 &:= (\mathbf{T}-\mathbf{R})\mathbf{T}_{\phi_2}.
\end{aligned}$$

Then, we write the costate equations (2.6) and (2.7) as

$$\begin{aligned}
\nabla\cdot(v_1,-v_2) &= v_{1_{x_1}}-v_{2_{x_2}}=G_1, \\
\nabla\cdot(v_2,v_1) &= v_{2_{x_1}}+v_{1_{x_2}}=G_2.
\end{aligned}$$

By taking the appropriate derivatives of both of sides of last system of equations we obtain the Poisson equations

$$\Delta v_1 = G_{1_{x_1}} + G_{2_{x_2}}, \tag{2.10}$$

$$\Delta v_2 = G_{2_{x_1}} - G_{1_{x_2}}. \tag{2.11}$$

In the similar way, using the state equations (2.4), (2.5) and the optimality conditions $w_1 f = v_1$ and $w_2 g = v_2$ and defining $F_1 := f - 1, \quad F_2 := g$, we obtain

$$\Delta u_1 = F_{1_{x_1}} - F_{2_{x_2}} = \frac{v_{1_{x_1}}}{w_1} - \frac{v_{2_{x_2}}}{w_2}, \tag{2.12}$$

$$\Delta u_2 = F_{1_{x_2}} + F_{2_{x_1}} = \frac{v_{1_{x_2}}}{w_1} + \frac{v_{2_{x_1}}}{w_2}. \tag{2.13}$$

In the next section we solve these systems of Poisson equations in a decoupled manner with an iterative way. Let us note that we chose $w_1 = w_2 = 200$ in the numerical implementation of the program at Fortran language.

3 Numerical Implementation

Although there are a few sophisticated methods to solve this type of system of equations numerically, we use finite-difference multigrid method. We first solve the above Poisson equations sequentially and then update the control variables along with the gradients provided by the optimality condition. The computational algorithm for the solution of this coupling system is given as follows:

- Suppose that at the k^{th} step, we have found f^k and g^k.
- Obtain $u^k = (u_1^k, u_2^k)$ from the decoupled state equations (2.12) and (2.13).
- Obtain v_1^k, v_2^k from the decoupled costate equations (2.10) and (2.11).
- Next get new controls (f^{k+1}, g^{k+1}) from the optimality conditions, (2.8), (2.9).
- Normalize controls and repeat the same process until the error condition is satisfied or a present number of iterations is achieved.

4 Computational Examples

4.1 Image Registration Quality Assessment Metrics

Referring to [7], we apply the following quality assessment metrics for our examples.

Sum of Squared Difference (SSD) Given reference image R, template image T, and nodal coordination $\boldsymbol{\xi}$, SSD is defined as

$$SSD = \frac{1}{\|T\|} \sum_{\boldsymbol{\xi} \in \Omega} (R(\boldsymbol{\xi}) - T(\phi(\boldsymbol{\xi})))^2,$$

which quantifies the difference between the registered template image T and reference image R, where $\|T\|$ is the total number of pixels in T and ϕ is a transformation function.

Warping Index Mean warping index [8],

$$\bar{\omega} = \frac{1}{\|T\|} \sum_{\boldsymbol{\xi} \in \Omega} \|\phi(\boldsymbol{\xi}) - \phi^*(\boldsymbol{\xi})\|,$$

is used as the registration quality metrics, where ϕ is the deformation field obtained after the image registration, ϕ^* is the ground truth of the deformation field, $\boldsymbol{\xi}$ is the coordinate of a nodal position, T is the template image, and $\|\phi(\boldsymbol{\xi}) - \phi^*(\boldsymbol{\xi})\|$ is the Euclidean's distance between $\phi(\boldsymbol{\xi})$ and $\phi^*(\boldsymbol{\xi})$.

Mean warping index is an appropriate metric to assess the overall quality of the registration result if the ground truth deformation field is available.

Masked Warping Index To properly reflect the quality of the image registration results, we need to exclude the homogeneous background area in the reference image R by imposing a binary mask in the process of computing the warping index.

Therefore, the masked mean warping index $\bar{\omega}^*$ is introduced here as

$$\bar{\omega}^* = \frac{1}{\|\Omega^*\|} \sum_{\boldsymbol{\xi} \in \Omega^*} \|\phi(\boldsymbol{\xi}) - \phi^*(\boldsymbol{\xi})\|. \tag{4.12}$$

4.2 Example 1: Synthetic Images of Elliptical Shape

The following example is implemented by the Lagrange Multiplier's method.

Example 1: The example is adopted from [17] which used a free form deformation registration method to register two disks of very different radius. Large deformation is a character of cardiac images.

Let reference image, $R(x, y)$ and the template image, $T(x, y)$ be given on the domain $\Omega = [0, 1] \times [0, 1]$ as follows:

$$R(x,y) = \begin{cases} 10, & d(x,y) \le 0; \\ 9.5 + 5(0.1 + 1.5d(x,y)), & 0 \le d(x,y) \le 2; \\ 25, & 2 \le d(x,y). \end{cases}$$

where

$$d(x,y) = \sqrt{1.6(x-30)^2 + (y-30)^2} - 12.$$

$$T(x,y) = \begin{cases} 10, & d(x,y) \le 0; \\ 9.5 + 5(0.1 + 3d(x,y)), & 0 \le d(x,y) \le 1; \\ 25, & 1 \le d(x,y). \end{cases}$$

where

$$d(x,y) = \sqrt{(x-35)^2 + 1.5(y-35)^2} - 7.$$

We used discrete images which have a resolution of 64 × 64 pixels. Figure 1 contains reference and template images and Figure 2 illustrates movement of the reference image towards the template image. The picture at the right bottom of the Figure 2 shows that iterated reference image is really close to the template image at the end of 230 iterations. Table 1 tells us the SSD is close to an optimal value at the end of 230 iterations, which is one of the achievements of our method.

Table 1: SSD and duration of implementation

Iterations	SSD with MG	MG Duration
1	1674.6	1 sec
2	908.5	1.1 sec
20	40.7	7 sec
120	6.4	38 sec
230	2.9	55 sec

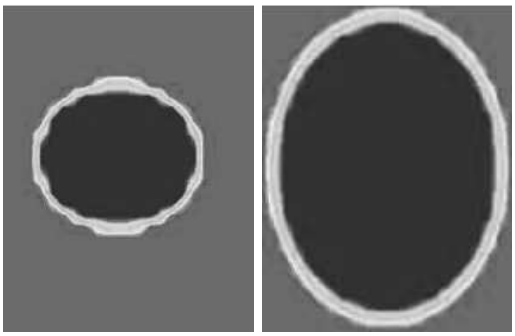

Figure 1: Reference and template images (left and right, respectively)

4.3 Example 2: Images Based on the Visible Human Project

4.3.1 Lagrange Multipler Method

The template image T is taken from the Visible Human Project [1]. The reference image is then formed by applying the known transformation (the ground truth shown in Fig. 3(e)) to the template image.

The initial SSD is 1047.65. After convergence, SSD is down to 14.8% of the initial SSD.

Fig. 3(f) shows the mask used to evaluate the masked mean/max warping index based on the segmentation of reference image R. The initial masked mean warping index is 0.6228, after registration, the masked mean warping index becomes 0.2386.

5 Summary and Conclusion

Nonrigid image registration is a significant branch of the image processing concept. It has broad application areas in medical and non-medical imaging. For instance, it can be used in analyzing local anatomical variations that exist between images acquired from different individuals or atlases. It can serve as a powerful tool for combining information from multiple sources, monitoring changes in an individual, detect tumors and locate disease, motion correction.

In this article we have presented a systematic method for the non-rigid registration of 2D images. The Lagrange multipliers method was used to solve the optimization problem.

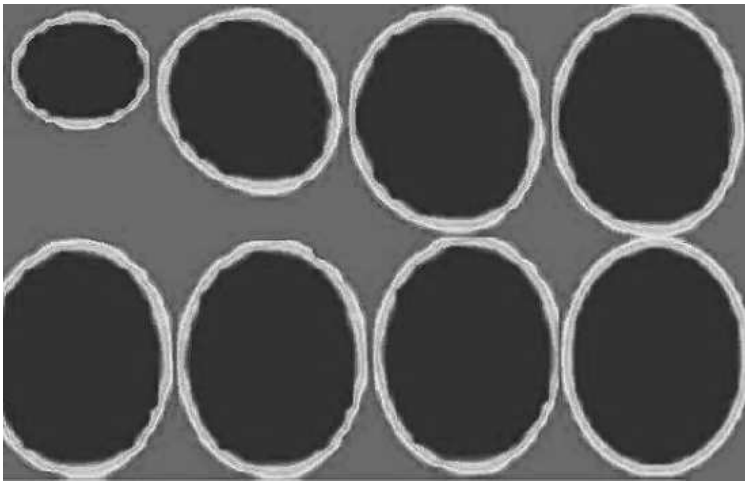

Figure 2: Movement of template image towards reference image

Table 2: Lagrange Multiplier Example 2 Result

Iterations	SSD	percentage
initial	1047.65	100%
1	924.38	88.2%
2	900.20	85.9%
20	787.45	75.1%
1000	155.55	14.8%

We solved the Poisson equations appearing in the optimality system by means of multigrid method. We applied our method to some 2D images. The method has also been extended to 3D images, the results will be reported in a different paper.

We implemented our algorithms in Fortran language. Computational examples given in the previous section were used to test the algorithms. Image registration experiments demonstrate the accuracy and efficiency of our registration techniques.

Acknowledgments

G. Liao and M. Akinlar are partially supported by NSF grants. The opinions expressed in this work do not represent the views of NSF.

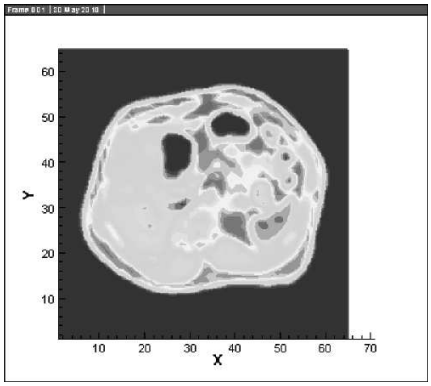

(a) Reference image.

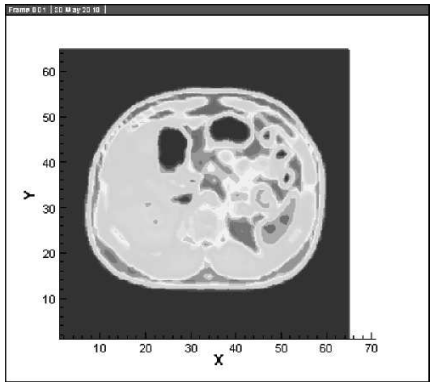

(b) Template image.

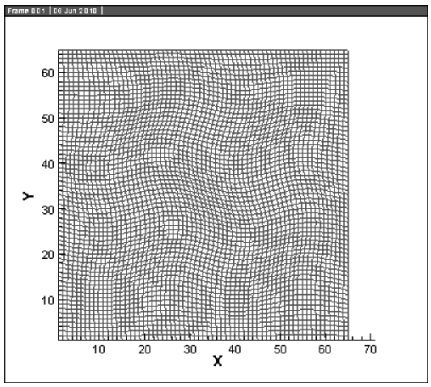

(c) Registered grid.

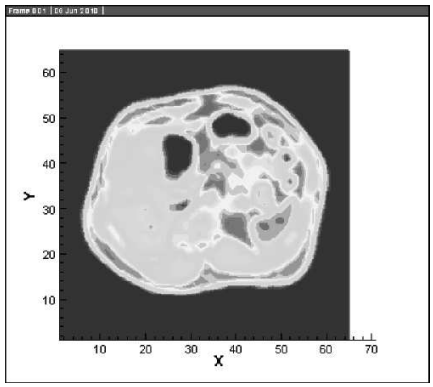

(d) Registered template image.

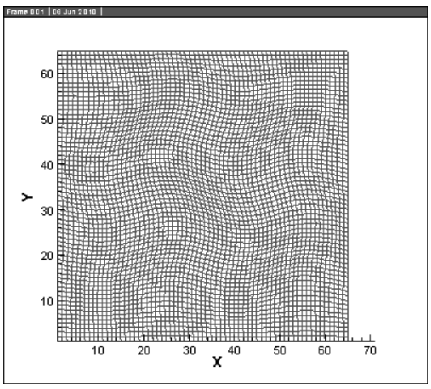

(e) Ground truth grid.

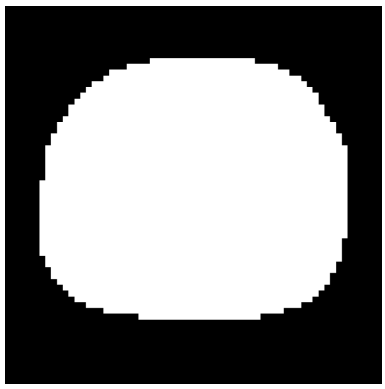

(f) Mask.

Figure 3: An example of registering a template image to reference image using Lagrange Multiplier method.

References

[1] Visible human project, http://www.nlm.nih.gov/research/visible/visible_human.html.

[2] R. Bajcsy and S. Kovačič, Multiresolution elastic matching. *Computer Vision, Graphics, and Image Processing,* **46**(1)(1989), 1-21.

[3] G.E. Christensen, R.D. Rabbitt, and M.I. Miller, Deformable templates using large deformation kinematics. *Image Processing, IEEE Transactions on,* **5**(10)(1996), 1435-1447.

[4] B. Fischer and J. Modersitzki, Curvature Based Image Registration. *Journal of Mathematical Imaging and Vision,* **18**(1)(2003), 81-85.

[5] M.D. Gunzburger and H.C. Lee, Analysis and approximation of optimal control problems for first-order elliptic systems in three dimensions. *Applied Mathematics and Computation,* **100**(1)(1999), 49-70.

[6] J.V. Hajnal, D.J. Hawkes, and D.L.G. Hill, *Medical image registration* (CRC, 2001).

[7] Chih-Yao Hsieh, *Nonrigid image registration by deformation based grid generation.* Ph.D. thesis, University of Texas at Arlington, December 2008.

[8] J. Kybic and M. Unser, Fast parametric elastic image registration. *Image Processing, IEEE Transactions on* **12**(11)(2003), 1427-1442.

[9] S.J. Latham, T. Varslot, and A. Sheppard, Automated registration for augmenting micro-CT 3D images. *ANZIAM Journal,* **50**.

[10] E. Lee and M. Gunzburger, An optimal control formulation of an image registration problem. *Journal of Mathematical Imaging and Vision,* **36**(1)(2010), 69-80.

[11] G. Liao, X. Cai, D. Fleitas, X. Luo, J. Wang, and J. Xue, Optimal control approach to data set alignment. *Applied Mathematics Letters,* **21**(9)(2008), 898-905.

[12] G. Liao, X. Cai, J. Liu, X. Luo, J. Wang, and J. Xue, Construction of differentiable transformations. *Applied Mathematics Letters,* **22**(10)(2009), 1543-1548.

[13] J. Liu, *New Developments Of The Deformation Method.* Ph.D. thesis, The University of Texas at Arlington, 2007.

[14] R.I. McLachlan and S. Marsland, Discrete mechanics and optimal control for image registration. *ANZIAM,* **48**(2007), 1-16.

[15] J.-P. Thirion, Image matching as a diffusion process: an analogy with Maxwell's demons. *Medical Image Analysis,* **2**(3)(1998), 243-260.

[16] E. Zeidler, *Nonlinear functional analysis and its applications: Variational methods and optimization.* (Springer, 1985).

[17] X. Zhuang, K. Rhode, R. Razavi, D.J. Hawkes, and S. Ourselin, Free-form deformations using adaptive control point status for whole heart MR segmentation. In *Proceedings of the 5th International Conference on Functional Imaging and Modeling of the Heart*, (Springer, 2009), page 311.